'89 KACC 1989. 10. 27~28

Speed and Efficiency Control of Induction Motors via Asymptotic Decoupling

Gyu-Sik Kim, In-Joong Ha, Myoung-Sam Ko, Dong-Il Kim, and Jeom-Geun Kim

Dept. of Control and Instrumentation Engineering,
Seoul National University, San 56-1, Shinrim-Dong,
Kwanak-ku, Seoul 151-742, Korea.

Abstract--In this paper, we attempt to control induction motors with high power efficiency as well as high dynamic performance by utilizing the recently developed theories: singular perturbation technique and noninteracting feedback control. Our controller does not need the transformation between a d-q synchronously rotating frame and a x-y stator-fixed frame. It is computationally quite simple. Furthermore, it does not depend on the rotor resistance. To illuminate the practical significance of our results, we present simulation and experimental results as well as mathematical performance analysis.

1. INTRODUCTION

Along with the rapid growth in microelectronics and power electronics technologies, various advanced control methods for ac motors have been successfully implemented in real time and shown to be useful in controlling induction motors with high dynamic performance. The controllers proposed in Ohnishi *et al.* (1985) can control the induction motors to behave like dc motors but can not decouple motor torque and rotor flux dynamically. Consequently, the changes in the rotor flux required for power efficiency control can degenerate the dynamic performance of the induction motors. On the other hand, the controllers proposed in Krzeminski (1987), Ho and Sen (1988), and Kim *et al.* (1989) can control the induction motors with rotor speed (or motor torque) and rotor flux linearly decoupled. The recently developed feedback linearization technique was utilized for decoupling of rotor speed (or motor torque) and rotor flux. Some experimental results are also presented in Kim *et al.* (1989).

In this paper, we propose a nonlinear feedback controller that can control the induction motors with high power efficiency as well as high dynamic performance. Our controller consists of three subcontrollers; a saturation current controller, a decoupling controller, and a well-known flux simulator. The saturation current controller is used for direct control of the stator currents. The decoupling controller decouples rotor speed (or motor torque) and rotor flux linearly. The well-known flux simulator is employed to estimate the rotor fluxes indirectly. During transients, the rotor fluxes are regulated to their rated values for maximal torque per ampere of stator current. Under steady state condition, the rotor fluxes are adjusted to keep the slip speed at the optimum value for maximal power efficiency. By virtue of decoupling of rotor flux and rotor speed, this can be successfully done without interfering rotor speed responses.

As mentioned above, induction motors with our controller can attain high dynamic performance and high power efficiency simultaneously. Like Krzeminski's controller in Krzeminski (1987), our controller does not need the transformation between a d-q synchronously rotating frame and a x-y stator-fixed frame. Like the controllers in Krzeminski (1987), Ho and Sen (1988), and Kim *et al.* (1989), ours can decouple rotor speed(or motor torque) and the rotor flux. In Krzeminski (1987) and Ho and Sen (1988), however, power efficiency was not considered. Our controller is computationally much simpler than the controllers in Krzeminski (1987) and Kim *et al.* (1989). Furthermore, our controller is less sensitive to variations of the machine parameters than the controllers in Krzeminski (1987) and Ho and Sen (1988) since ours do not depend on the rotor resistance which varies most widely as the machine temperature rises. To illuminate the practical significance of our results, we present simulation and experimental results as well as mathematical performance analysis.

2. CONTROLLER DESIGN

In this section, we describe our approach to control of the induction motors whose dynamic equations are described, in the x-y stator-fixed frame, as

$$
\begin{aligned}
\dot{i}_{xs} &= -a_1 i_{xs} + a_2\phi_{xr} + p a_3 w_r \phi_{yr} + a_0 V_{xs},\\
\dot{i}_{ys} &= -a_1 i_{ys} - p a_3 w_r \phi_{xr} + a_2\phi_{yr} + a_0 V_{ys},\\
\dot{\phi}_{xr} &= -a_4\phi_{xr} - p w_r \phi_{yr} + a_5 i_{xs},\\
\dot{\phi}_{yr} &= -a_4\phi_{yr} + p w_r \phi_{xr} + a_5 i_{ys},\\
\dot{w}_r &= -a_6 w_r + a_7(T_e - T_L),
\end{aligned}
\tag{1}
$$

where $u = [V_{xs}\ \ V_{ys}]^T$ is the control input and T_e is the generated torque given by

$$T_e = K_T(\phi_{xr}\ i_{ys} - \phi_{yr}\ i_{xs}) \quad . \tag{2}$$

Here, the constants K_T and a_i, $i = 1,\cdots,7$ are the parameters of the induction motor. See the Nomenclature for the symbols and notations that appear frequently in our developments.

In many industrial applications of induction motors, high dynamic performance and high power efficiency are equally important. It is shown in Kusko and Galler (1983) that if w_r and T_L are constant, (a) there is an optimal slip speed w_{sl}^* that leads to maximal power efficiency and (b) the optimal slip speed is a function (say, f) of w_r. The slip speed w_{sl} can be expressed in terms of the generated torque and rotor fluxes (Joetten and Maeder, 1983):

$$w_{sl} = (a_5/K_T)\ T_e\ /\ \phi\ , \tag{3}$$

where $\phi = \phi_{xr}^2 + \phi_{yr}^2$. When w_r and T_L are constant, we can write the slip speed as

$$w_{sl} = (a_5/K_T)[(a_6/a_7)w_r + T_L]/\phi. \tag{4}$$

This follows easily from (3) and the last equation of (1). From (4), we see that, if ϕ is regulated to the value $(a_5/K_T)\ [(a_6/a_7)w_r + T_L]\ /\ w_{sl}^*$, the slip speed can be kept at its optimal value and hence maximal power efficiency can be achieved in the steady state. For these reasons, the output to be controlled is chosen as

$$y = [y_1\ \ y_2]^T = [w_r\ \ \phi]^T. \tag{5}$$

If a high-gain or bang-bang current controller is employed, the stator currents i_{xs}, i_{ys} can be directly controlled. Here, we propose a saturation current controller:

$$u = \begin{bmatrix} V_{xs} \\ V_{ys} \end{bmatrix} = \begin{bmatrix} K\ \mathrm{sat}(\ (\hat{u}_1 - i_{xs})/\delta\ ) \\ K\ \mathrm{sat}(\ (\hat{u}_2 - i_{ys})/\delta\ ) \end{bmatrix}, \tag{6}$$

where K, δ are some positive constants, $\hat{u} = [\hat{u}_1, \hat{u}_2]^T$ is the new input, and

$$\mathrm{sat}(\eta) \triangleq \begin{cases} \eta\ , & |\eta| \le 1\ , \\ \eta/|\eta|\ , & |\eta| \ge 1\ . \end{cases} \tag{6}'$$

The above saturation current controller may be viewed as a continuous approximation of the discontinuous bang-bang current controller. Furthermore, the high-gain current controller actually functions as a saturation current controller in face of physical limitations. Later, we will discuss roles of the free parameters K and δ.

When the stator currents are directly controlled by the above saturation current controller in (6), the dynamic equations of the induction motor in (1) and (2) can be approximated to

$$\begin{aligned} \dot{\phi}_{xr} &= -a_4\ \phi_{xr} - p\ w_r\ \phi_{yr} + a_5\ \hat{u}_1, \\ \dot{\phi}_{yr} &= -a_4\ \phi_{yr} + p\ w_r\ \phi_{xr} + a_5\ \hat{u}_2, \\ \dot{w}_r &= -a_6 w_r + a_7 K_T(\phi_{xr}\hat{u}_2 - \phi_{yr}\hat{u}_1) - a_7 T_L. \end{aligned} \tag{1}'$$

Then, one can easily check that if $\phi \neq 0$, the reduced system consisting of (1)' and (5) with $T_L = 0$ satisfies the well-known conditions for decoupling in Singh and Rugh (1972), Ha (1988), and other literature. Following directly the computation procedures in Singh and Rugh (1972) and Ha (1988), one can find the nonlinear feedback controller $\hat{u}$ that decouples the reduced system consisting of (1)' and (5).

$$\hat{u} = \frac{1}{\phi}\begin{bmatrix} -\phi_{yr} & \phi_{xr} \\ \phi_{xr} & \phi_{yr} \end{bmatrix} \bar{u}\ , \tag{7}$$

where $\bar{u} = [\bar{u}_1\ \ \bar{u}_2]^T$ is the new input. As the result, the input-output dynamic characteristics of the closed-loop system given by (1)', (5), and (7) are determined by the following linear decoupled system.

$$\begin{aligned} \dot{w}_r &= -a_6\ w_r + a_7\ (K_T\ \bar{u}_1 - T_L), \\ \dot{\phi} &= -2a_4\ \phi + 2a_5\ \bar{u}_2, \\ \bar{y}_1 &= w_r, \quad \bar{y}_2 = \phi. \end{aligned} \tag{8}$$

In order to obtain desirable transient and steady state performances, the new inputs $\bar{u}_1$, $\bar{u}_2$ are chosen as the following IP (Integral-Proportional) controllers.

$$\begin{aligned} \bar{u}_1 &= -k_{p1}\ w_r + k_{i1}\int_0^t (w_r^* - w_r)dt, \\ \bar{u}_2 &= -k_{p2}\ \phi + k_{i2}\int_0^t (\phi^* - \phi)dt, \end{aligned} \tag{9}$$

where the constants k_{pj}, k_{ij}, $j = 1, 2$ are controller gains and w_r^*, ϕ^* represent the command inputs for w_r, ϕ, respectively.

Letting $\bar{z} = [\bar{z}_1^T\ \bar{z}_2^T]^T$, where $\bar{z}_1 = [\bar{z}_{11}\ \bar{z}_{12}]^T = [w_r\ \int_0^t (w_r^* - w_r)dt]^T$ and $\bar{z}_2 = [\bar{z}_{21}\ \bar{z}_{22}]^T = [\phi\ \int_0^t (\phi^* - \phi)dt]^T$, the closed-loop system given by (8) and (9) can be represented in the state space as

$$\dot{\bar{z}} = \begin{bmatrix} \dot{\bar{z}}_1 \\ \dot{\bar{z}}_2 \end{bmatrix} = \begin{bmatrix} A_1\ \bar{z}_1 + b\ w_r^* + L\ T_L \\ A_2\ \bar{z}_2 + b\ \phi^* \end{bmatrix}, \tag{10}$$

$$\bar{y}_i = c\ \bar{z}_i\ , \quad i = 1, 2,$$

where the detailed structures of A_i, $i = 1, 2$, b, c, and L are given in Appendix A. Its block diagram representation is shown in Fig. 1.

Note that the responses of rotor speed and rotor flux are dynamically linear and decoupled. The rotor flux can be adjusted to achieve maximal power efficiency without interfering rotor speed responses. The control strategy of ϕ for maximal power efficiency will be presented in Section 4.

Remark 1. By appropriate choice of the controller gains in (9), the linear system (10) can be made BIBS (Bounded Input Bounded State) stable. One can easily check that although the decoupled linear system (8) has less dimension than the reduced system (1)', BIBS stability of the linear system (10) always implies BIBS stability of the closed-loop system given by (1)', (7), and (9).

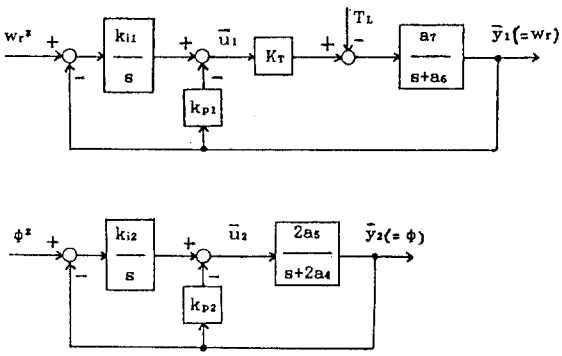

Fig. 1. The block diagram of the decoupled linear system (10).

Thus, the controller consisting of (6), (7), and (9) can control the induction motors with high dynamic performance and high power efficiency. Besides, our controller is computationally simple. In contrast to most of previously known field oriented control methods, it does not need the transformation between a d-q synchronously rotating frame and a x-y stator-fixed frame. It is robust with respect to variations of the machine parameters since it depends on none of the machine parameters.

The proposed controller needs information of rotor fluxes. It is more cost-effective and practical to estimate indirectly rotor fluxes than to install flux sensors on the stator. For this reason, we adopt the following well-known rotor flux simulator based on the stator circuit:

$$\hat{\phi}_{xr} = (a_0/a_3)\int_0^t (V_{xs}-R_s i_{xs})dt-(1/a_3)i_{xs}+\hat{u}_x,$$
$$\hat{\phi}_{yr} = (a_0/a_3)\int_0^t (V_{ys}-R_s i_{ys})dt-(1/a_3)i_{ys}+\hat{u}_y. \qquad (11)$$

Here, $\hat{\phi}_{xr}$, $\hat{\phi}_{yr}$ represent the estimated values of ϕ_{xr}, ϕ_{yr} and $\hat{u}_x$, $\hat{u}_y$ represent the estimated values of $u_x = \phi_{xr}(0) + i_{xs}(0)/a_3$, $u_y = \phi_{yr}(0) + i_{ys}(0)/a_3$, respectively. It can be easily seen that if $\hat{u}_x = u_x$ and $\hat{u}_y = u_y$, then, $\hat{\phi}_{xr} = \phi_{xr}$, $\hat{\phi}_{yr} = \phi_{yr}$, $t \geq 0$. In this paper, we propose the following estimation method for $\hat{u}_x$, $\hat{u}_y$. Under no load condition (i.e. $T_L = 0$), control the stator currents i_{xs}, i_{ys} directly by the saturation current controller in (6) with $\hat{u}_1 = I_0$ (a nonzero constant) and $\hat{u}_2 = 0$. After sufficient time, take $\hat{u}_x$, $\hat{u}_y$ by

$$\hat{u}_x = (1/a_3 + M)\, I_0, \qquad \hat{u}_y = 0, \qquad (12)$$

respectively. This method can yield fairly good estimation of u_x, u_y since the dynamic equations of the induction motor in (1) and (2) with the saturation current controller in (6) can be approximated to (1)' (see (21) in Section 3) and then

$$i_{xs}^s = I_0, \quad \phi_{xr}^s = MI_0, \quad i_{ys}^s = \phi_{yr}^s = 0. \qquad (13)$$

The decoupling controller in (7) and the IP controllers in (9) need be modified so as to be based on the estimated values of rotor fluxes.

$$\tilde{u} = \frac{1}{\hat{\phi}}\begin{bmatrix} -\hat{\phi}_{yr} & \hat{\phi}_{xr} \\ \hat{\phi}_{xr} & \hat{\phi}_{yr} \end{bmatrix}\tilde{u}, \qquad (7)'$$

$$\tilde{u}_1 = -k_{p1}\, w_r + k_{i1}\int_0^t (w_r^* - w_r)dt,$$
$$\tilde{u}_2 = -k_{p2}\, \hat{\phi} + k_{i2}\int_0^t (\phi^* - \hat{\phi})dt, \qquad (9)'$$

where $\hat{\phi}$ is defined by $\hat{\phi} = \hat{\phi}_{xr}^2 + \hat{\phi}_{yr}^2$. The final form of our controller consists of three subcontrollers; the saturation current controllers in (6), the rotor flux simulator in (11), and the asymptotically decoupling controller in (7)' and (9)'.

Remark 2. A drawback of the rotor flux simulator in (11) is poor behavior at low rotor speeds. The new flux observers based on the rotor circuit in Verghese and Sanders (1988) may replace the rotor flux simulator in (11). However, these new observers may be more sensitive to the variations of the rotor resistance than the flux simulator in (11). Note that the rotor flux simulator in (11) does not depend on the rotor resistance.

3. PERFORMANCE ANALYSIS

Since the rotor flux simulator presented at the end of Section 2 can estimate ϕ_{xr}, ϕ_{yr} with fairly good accuracy, we assume that

(A.1) $\hat{\phi}_{xr} = \phi_{xr}$, $\hat{\phi}_{yr} = \phi_{yr}$, $t \geq 0$.

Let $x = [x_1 \cdots x_7]^T$ where $x_1 = i_{xs}$, $x_2 = i_{ys}$, $x_3 = \phi_{xr}$, $x_4 = \phi_{yr}$, $x_5 = w_r$, $x_6 = \int_0^t (w_r^* - w_r)dt$, and $x_7 = \int_0^t (\phi^* - \phi)dt$. Let $u^* = [u_1^* \; u_2^*]^T = [w_r^* \; \phi^*]^T$.

For technical simplicity, we assume that

(A.2) For each $u_i^*:[0,\infty) \to \Omega_i$, $i = 1, 2$, $T_L:[0,\infty) \to \Omega_T$, and $x(0) \in \Omega_x$, the closed-loop system (1), (2), (5), (6), (11), (7)' and (9)' has a unique solution $x:[0,\infty) \to \Omega_x$.

That is, we assume that the system (1), (2), (5), (6), (11), (7)' and (9)' has a well-defined solution and is BIBS (Bounded Input - Bounded State). See Remark 3 for further comments on (A.2).

Let $\varepsilon = [\varepsilon_1 \; \varepsilon_2]^T$ where $\varepsilon_i = \hat{u}_i - x_i$, $i = 1, 2$. Let $z = [z_1^T \; z_2^T]^T$, where $z_1 = [z_{11} \; z_{12}]^T = [x_5 \; x_6]^T$ and $z_2 = [z_{21} \; z_{22}]^T = [x_3^2 + x_4^2 \;\; x_7]^T$. Then, the derivatives of ε, z along the solution trajectories of the system (1), (2), (5), (6), (11), (7)' and (9)' can be written as

$$\dot{\varepsilon} = \begin{bmatrix}\dot{\varepsilon}_1 \\ \dot{\varepsilon}_2\end{bmatrix} = \begin{bmatrix} -a_1\varepsilon_1 - a_0 K \mathrm{sat}(\varepsilon_1/\delta) + g_1(x,u^*,T_L) \\ -a_1\varepsilon_2 - a_0 K \mathrm{sat}(\varepsilon_2/\delta) + g_2(x,u^*,T_L) \end{bmatrix}, \qquad (14)$$

$$\dot{z} = \begin{bmatrix}\dot{z}_1 \\ \dot{z}_2\end{bmatrix} = \begin{bmatrix} A_1 z_1 + b\, w_r^* + h_1(x)\varepsilon + L\, T_L \\ A_2 z_2 + b\, \phi^* + h_2(x)\varepsilon \end{bmatrix}, \qquad (15)$$

$$y_i = c\, z_i, \quad i = 1, 2,$$

where the detailed structures of g_i, h_i, $i = 1, 2$, are given in Kim, G. S. *et al.* (1989).

By (A.2) and the continuity of g_i, h_i, $i = 1, 2$, there exist positive constants d_{ij}, $i = 1, 2$, $j = 1, 2$ such that

$$|g_i(x,u^*,T_L)| \le d_{i1}, \quad \|h_i(x)\| \le d_{i2}, \quad i = 1,2. \tag{16}$$

Simple calculations show that if the controller gains are chosen as $k_{P1} > -B/K_T$ and $k_{P2} > -1/M$, all eigenvalues of A_1 and A_2 have negative real parts. Therefore, we can assume

(A.3) A_1 and A_2 are stable matrices.

Let $Q_i \in R^{2\times 2}$ be positive definite symmetric matrices. By (A.3), there exist positive definite symmetric matrices $P_i \in R^{2\times 2}$ satisfying

$$A_i^T P_i + P_i A_i = -Q_i, \quad i = 1,2. \tag{17}$$

Finally, we need the following notations in order to state our result on the input-output dynamic behavior of the closed-loop system in (1), (2), (5), (6), (11), (7)' and (9)'.

$$\begin{aligned} d_{3i} &= (d_{i1}\,\delta/a_1)^{1/2}/2, \\ d_{4i} &= 2\lambda_M(P_i)\|P_i\|d_{i2}(d_{31}+d_{32})/\ \lambda_m(P_i)\lambda_m(Q_i), \\ d_{5i} &= 2\|P_i\|d_{i2}(|\varepsilon_1(0)|+|\varepsilon_2(0)|) \\ &\quad /\lambda_m(P_i)(\lambda_m(Q_i)/\lambda_M(P_i) - 2a_1), \\ m_{1i} &= \lambda_m(Q_i)/2\lambda_M(P_i), \quad i = 1, 2. \end{aligned} \tag{18}$$

Theorem 1 Suppose that (A.1)-(A.3) are satisfied. Then, the controller given by (6), (11), (7)', and (9)' with $K \ge \max(d_{11}, d_{21})/a_0$ guarantees that, for $i = 1, 2$ and for $t \ge 0$,

$$|\varepsilon_i(t)| \le d_{3i} + |\varepsilon_i(0)|\, e^{-a_1 t}, \tag{19}$$

$$|y_i(t) - \bar{y}_i(t)| \le d_{4i} + d_{5i}e^{-a_1 t} - (d_{4i} + d_{5i})e^{-m_{1i}t}. \tag{20}$$

and that if u^* and T_L are constant,

$$\phi^s = \phi^* \quad \text{and} \quad w_r^s = w_r^*. \tag{21}$$

Theorem 1 states that the output responses of the induction motor with our controller asymptotically follow those of the decoupled linear system (10) with bounded errors. By (18), $d_{3i} \to 0$ and $d_{4i} \to 0$, $i = 1, 2$ as $\delta \to 0$. Consequently, from (19)-(20), we see that $\lim_{\delta \to 0}|\varepsilon_i| = 0$ and $\lim_{\delta \to 0}|y_i - \bar{y}_i| = 0$, $i = 1, 2$, as $\delta \to 0$. Note that as $\delta \to 0$, the saturation current controller in (6) tends to be a bang-bang current controller. Thus, Theorem 1 suggests that the bang-bang current controller may provide better control performances than the saturation current controller. However, the bang-bang current controller can cause undesirable chattering phenomena.

See Kim, G. S. *et al.* (1989) for the detailed proof of Theorem 1.

Remark 3 By (A.2), we priorly assumed that the closed-loop system (1), (2), (5), (6), (11), (7)' and (9)' is BIBS. By (A.3), the decoupled linear system (10) is also BIBS. Under these assumptions, Theorem 1 shows that the output responses of the closed-loop system (1), (2), (5), (6), (11), (7)' and (9)' can be made to follow the desired ones (i.e. the output responses of the decoupled linear system (10)) as closely as desired by decreasing the free parameter δ of the saturation current controller in (6). The assumption (A.2) can be removed by imposing restrictions on the allowable sizes of Ω_1, Ω_2, Ω_T, and $|x(0)|$. However, the statement and proof of Theorem 1 gets extremely complicated without much gain.

4. POWER EFFICIENCY CONTROL

In this section, we show that high power efficiency as well as high dynamic performance can be easily achieved by utilizing these features of our controller. In Section 2, we have seen that, when T_L and w_r are constant, w_{sl} is inversely related to ϕ (See the equation (4)) and that w_{sl}^* is a function of w_r. The function is assumed to be known a-priori. It is usually obtained experimentally rather than analytically.

Theorem 2. Assume that all hypotheses of Theorem 1 are satisfied. If w_r^* and T_L are constant, change the rotor flux command ϕ^* as

$$\phi^* = \begin{cases} \phi_r, & \text{until the closed-loop system (1), (2), (5), (6), (11), (7)' and (9)' reaches the steady state,} \\ a_4\phi_r\ \tilde{u}_1^s/\tilde{u}_2^s w_{sl}^*, & \text{if the closed-loop system (1), (2), (5), (6), (11), (7)', and (9)' with } \phi^*=\phi_r \text{ reaches the steady state,} \end{cases} \tag{22}$$

where ϕ_r denotes the rated value of ϕ. Then,

$$\left|\frac{w_{sl}^s - w_{sl}^*}{w_{sl}^*}\right| \le \frac{k_{i1}\ d_{41}}{|\tilde{u}_1^s|} + \frac{k_{i2}\ a_5\ d_{42}}{a_4\ \phi_r} + \frac{k_{i1}\ k_{i2}\ a_5\ d_{41}\ d_{42}}{a_4\ \phi_r\ |\tilde{u}_1^s|}. \tag{23}$$

We have chosen ϕ^* as a piecewise constant function. However, rotor speed responses will be little affected by such a step change in ϕ^* since the input-output dynamic characteristics of the induction motor with our controller closely follow those of the decoupled linear system (10), as has been shown in Theorem 1. Note that, during transients, the rotor fluxes are regulated to their rated values. This is to obtain maximum possible torque per ampere of stator current. Theorem 2 states that if ϕ^* is chosen as (22), the slip speed can be kept around the optimal slip speed in the steady state. From (23), we see that $w_{sl} \to w_{sl}^*$ as $\delta \to 0$.

See Kim, G. S. *et al.* (1989) for detailed proof of Theorem 2.

5. SIMULATION AND EXPERIMENTAL RESULTS

The performances of our control scheme developed in the preceding sections were studied through simulations and experiments. For experimental work, we have chosen a squirrel-cage induction motor. Its motor data are listed in Table 1. For load test, the induction motor was coupled with a 2.2 kW dc generator. The microprocessor-based control system designed for the induction motor is shown in Fig. 2.

Based on the decoupled linear system (10), we chose the controller gains as

$K = 140$, $k_{i1} = 1.275$, $k_{p1} = 0.228$,

$\delta = 0.05$, $k_{i2} = 187.032$, $k_{p2} = 9.291$. (24)

we have assumed in our simulations and experiments that $w_{si}^* = 30$, 70 rpm for $w_r^* = 650$, 1400 rpm, respectively.

Nameplate data
220V 60Hz
3-phase
delta-connected
4 poles
rated power 2.2kW
rated speed 1750rpm
rated rotor flux 0.48Wb
rated current 8.82A(rms)

Nominal parameters	
R_s	0.687Ω
R_r	0.842Ω
L_s	83.97mH
L_r	85.28mH
M	81.36mH
J	0.03Kgm²
B	0.01Kgm²/s
σ	0.0756

Table 1. Motor data of the induction motor chosen for simulation study.

In this situation, w_r^* was step-changed from 650 rpm to 1400 rpm. To provide maximal power efficiency in the steady state, ϕ^* was adjusted according to (35). The simulation and experimental results for this case are shown in Fig. 3 (a) and (b). Observe that the step change in ϕ^* made for power efficiency does not disturb the rotor speed response at all, while the steady state value of the slip speed approaches 70 rpm(the optimal slip speed for maximal power efficiency at $w_r = 1400$ rpm). Next, we applied the rated load torque 12 Nm for 1 second at $w_r = 1200$ rpm and $\phi = 0.23$ Wb². The simulation and experimental results in Fig. 4 (a) and (b) show that the rotor flux response is not affected by the load torque while the rotor speed promptly recovers its commanded value.

The simulation and experimental results shown in Fig. 3 and Fig. 4 demonstrate that our control scheme is useful in controlling induction motors with high power efficiency as well as high dynamic performance. As can be seen from Fig. 3 and Fig. 4, the experimental results agree well with the simulation results. Slight differences between the simulation and experimental results are unavoidable due to imperfect hardware

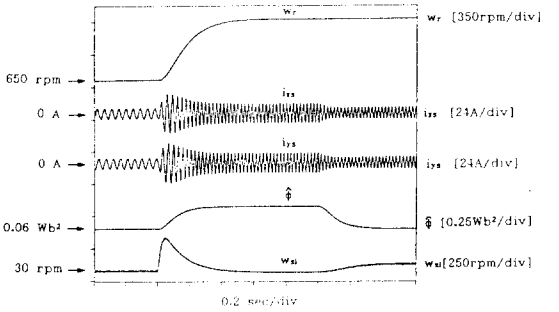

Fig. 3. (a) Simulation results

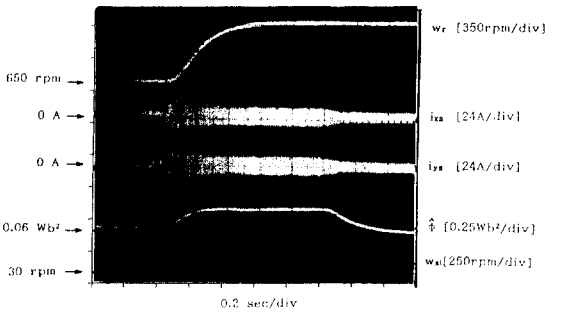

Fig. 3. (b) Experimental results for the case of step change in rotor speed command from 650 rpm to 1400 rpm.

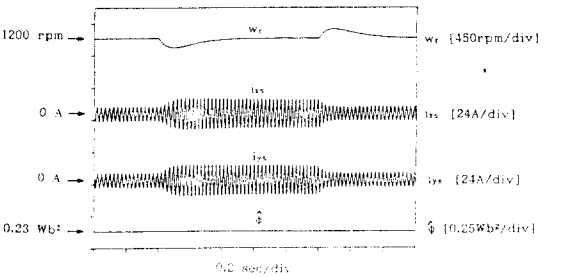

Fig. 4. (a) Simulation results

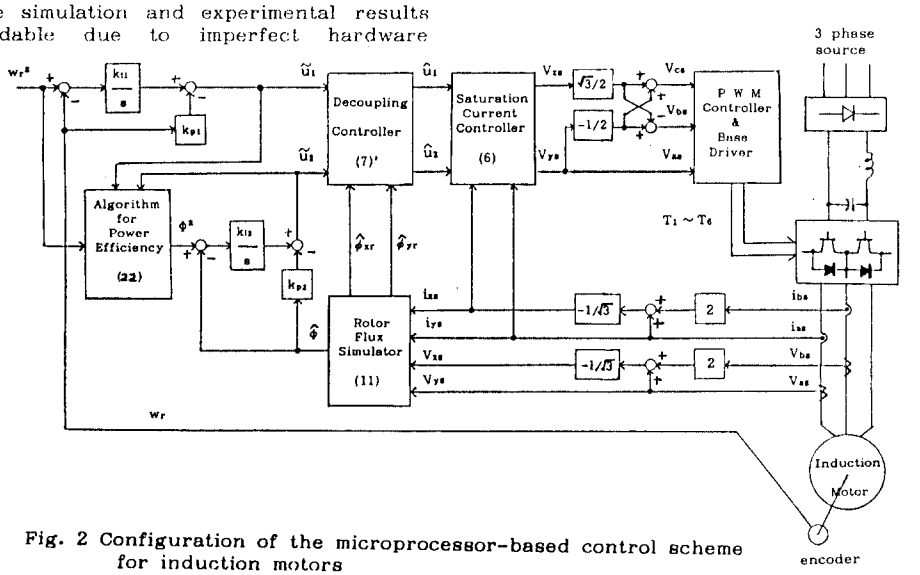

Fig. 2 Configuration of the microprocessor-based control scheme for induction motors

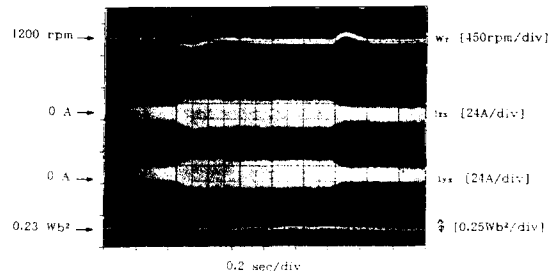

Fig. 4. (b) Experimental results for a rectangular load torque.

implementation, some uncertainties in the motor data, and etc.

6. CONCLUSION

Our power efficiency control method needs the prior-knowledge of optimal slip speeds at various rotor speeds. This extra labor may be avoided by employing such an on-line search method for optimal slip speed as the one proposed by Kirschen *et al.* (1987). In Kirschen *et al.* (1987), the flux command is continuously adjusted until measured power efficiency reaches the maximum. In our control scheme, this can be done without deteriorating the dynamic performance of the rotor speed.

The underlying approach taken in this paper can be viewed as an extension of the simplified feedback linearization technique proposed by Ha *et al.* (1989) in that a saturation type controller has been utilized for the simplified design process instead of the usual high gain feedback controller. The underlying approach should be applicable to other industrial systems.

Nomenclature

a_0	$1/\sigma L_s$
a_1	$a_0(R_s + M^2R_r/L_r^2)$
a_2	a_0MR_r/L_r^2
a_3	a_0M/L_r
a_4	R_r/L_r
a_5	MR_r/L_r
a_6	B/J
a_7	$1/J$
T_L	external load torque
$\|x\|$	Euclidean norm of $x \in R^n$
$\|A\|$	induced norm of a matrix A
x^T	transpose of a vector x
v^s	steady state value of the variable v
$\Omega_1,\Omega_2,\Omega_T$	compact subsets of R
Ω_x	compact subset of R_7 such that $\Omega_x \cap \{x \in R_7: x_3^2+x_4^2=0\}$ is empty
$\lambda_m(Q)(\lambda_M(Q))$	minimum(maximum) eigenvalue of a symmetric matrix Q

Appendix A

(1) A_i, i = 1, 2, b, c, and L in (10)

$$A_1 = \begin{bmatrix} -a_6 - K_T a_7 k_{p1} & K_T a_7 k_{i1} \\ -1 & 0 \end{bmatrix}, \quad A_2 = \begin{bmatrix} -2a_4 - 2a_5 k_{p2} & 2a_5 k_{i2} \\ -1 & 0 \end{bmatrix},$$

$$b = [0 \quad 1]^T, \quad c = [1 \quad 0], \quad L = [-a_7 \quad 0]^T.$$

REFERENCES

[1] Ha, I. J.(1988). The standard decomposed system and noninteracting feedback control of nonlinear systems. *SIAM J. of Contr. and Optimiz.*, **26**, 1235-1249.

[2] Ha, I. J., A. K. Tugcu, and N. M. Boustany (1989). Feedback Linearizing Control of Vehicle Longitudinal Acceleration. *IEEE Trans. Automat. Contr.*, **AC-34**, 689-698.

[3] Ho, E. Y. Y. and P. C. Sen (1988). Decoupling control of induction motor drives. *IEEE Trans. Ind. Elec.*, **IE-35**, 253-262.

[4] Joetten, R. and G. Maeder (1983). Control methods for good dynamic performance induction motor drives based on current and voltage as measured quantities. *IEEE Trans. Ind. Appl.*, **IA-19**, 356-363.

[5] Kim, D. I., M. S. Ko, and I. J. Ha (1989). Linear decoupling control of rotor speed and rotor flux in induction motor for high dynamic performance and maximal power efficiency. *Int. J. Contr.*, to appear.

[6] Kim, G. S., I. J. Ha, M. S. Ko, D. I. Kim, and J. W. Park (1989). Speed and efficiency control of induction motors via asymptotic decoupling. *20th Annual IEEE PESC Conf. 931-938.*

[7] Kirschen, D. S., D. W. Novotny, and T. A. Lipo (1987). Optimal efficiency control of an induction motor drive. *IEEE Trans. Energy Conversion*, **EC-2**, 70-75, 1987.

[8] Krzeminski, Z. (1987). Nonlinear control of induction motor. *Proc. 10th IFAC World Congress on Automatic Control*, Munich.

[9] Kusko, A. and D. Galler (1983). Control means for minimization of losses in AC and DC motor drives. *IEEE Trans. Ind. Appl.*, **IA-19**, 561-570.

[10] Liu, T. H., C. M. Young, and C. H. Liu (1988). Microprocessor-based controller design and simulation for a permanent magnet synchronous motor drive. *IEEE Trans. Ind. Elec.*, **IE-35**, 516-523.

[11] Nandam, P. K. and P. C. Sen (1986). A Comparative study of proportional-integral(P-I) and integral-proportional(I-P) controllers for dc motor drives. *Int. J. Contr.*, **44**, 283-297.

[12] Ohnishi, K., H. Suzuki, K. Miyachi, and M. Terashima (1985). Decoupling control of secondary flux and secondary current in induction motor drive with controlled voltage source and its comparison with volts/hertz control. *IEEE Trans. Ind. Appl.*, **IA-21**, 241-246.

[13] Singh, S. N. and W. J. Rugh (1972). Decoupling in a class of nonlinear systems by state variable feedback. *ASME J. Dynam. Syst., Measurement Contr.*, **94**, 323-329.

[14] Verghese, G. C. and S. R. Sanders (1988). Observers for flux estimation in induction machines. *IEEE Trans. Ind. Elec.*, **IE-35**, 85-94.